COMPARISON OF $\pi^{\pm}$, $K^{\pm}$ AND p, $\bar{p}$ PRODUCTION IN THE CENTRAL RAPIDITY REGION IN HADRON–HADRON COLLISIONS AND IN e^+e^- ANNIHILATION

H. AIHARA [a], M. ALSTON-GARNJOST [b], R.E. AVERY [b], A. BARBARO-GALTIERI [b], A.R. BARKER [c], A.V. BARNES [b], B.A. BARNETT [d], D.A. BAUER [c], H.-U. BENGTSSON [e], D.L. BINTINGER [f], G.J. BOBBINK [g], T.S. BOLOGNESE [b], A.D. BROSS [b], C.D. BUCHANAN [e], A. BUIJS [h], D.O. CALDWELL [c], A.R. CLARK [b], G.D. COWAN [b], D.A. CRANE [d], O.I. DAHL [b], K.A. DERBY [b], J.J. EASTMAN [b], P.H. EBERHARD [b], T.K. EDBERG [b], A.M. EISNER [i], R. ENOMOTO [a], F.C. ERNÉ [h], T. FUJII [a], J.W. GARY [b], W. GORN [j], J.M. HAUPTMAN [k], W. HOFMANN [b], J.E. HUTH [b], J. HYLEN [d], T. KAMAE [a], H.S. KAYE [b], K.H. KEES [f], R.W. KENNEY [b], L.T. KERTH [b], Winston KO [l], R.I. KODA [e], R.R. KOFLER [m], K.K. KWONG [j], R.L. LANDER [l], W.G.J. LANGEVELD [j], J.G. LAYTER [j], F.L. LINDE [h], C.S. LINDSEY [j], S.C. LOKEN [b], A. LU [c], X-Q. LU [d], G.R. LYNCH [b], R.J. MADARAS [b], K. MAESHIMA [l], B.D. MAGNUSON [i], J.N. MARX [b], G.E. MASEK [f], L.G. MATHIS [b], J.A.J. MATTHEWS [d], S.J. MAXFIELD [m], S.O. MELNIKOFF [j], E.S. MILLER [f], W. MOSES [b], R.R. McNEIL [l], P. NEMETHY [n], D.R. NYGREN [b], P.J. ODDONE [b], H.P. PAAR [h], D.A. PARK [e], S.K. PARK [k], D.E. PELLET [l], M. PRIPSTEIN [b], M.T. RONAN [b], R.R. ROSS [b], F.R. ROUSE [b], K.A. SCHWITKIS [c], J.C. SENS [h], G. SHAPIRO [b], M.D. SHAPIRO [b], B.C. SHEN [j], W.E. SLATER [e], J.R. SMITH [l], J.S. STEINMAN [e], M.L. STEVENSON [b], D.H. STORK [e], M.G. STRAUSS [e], M.K. SULLIVAN [i], T. TAKAHASHI [a], J.R. THOMPSON [f], N. TOGE [a], S.TOUTOUNCHI [m], R. van TYEN [b], B. VAN UITERT [h], G.J.VANDALEN [j], R.R. van DAALEN WETTERS [e], W. VERNON [f], W. WAGNER [b], E.M. WANG [b], Y.X. WANG [c], M.R. WAYNE [e], W.A. WENZEL [b], J.T. WHITE [f], M.S.C. WILLIAMS [l], Z.R. WOLF [b], H. YAMAMOTO [b], S.J. YELLIN [c], C. ZEITLIN [l] and W-M. ZHANG [d]

[a] *University of Tokyo, Tokyo 113, Japan*
[b] *Lawrence Berkely Laboratory, University of California, Berkely, CA 94720, USA*
[c] *University of California, Santa Barbara, CA 93106, USA*
[d] *Johns Hopkins University, Baltimore, MD 21218, USA*
[e] *University of California, Los Angeles, CA 90024, USA*
[f] *University of California, San Diego, CA 92093, USA*
[g] *Carnegie–Mellon University, Pittsburgh, PA 15213, USA*
[h] *National Institute for Nuclear and High Energy Physics, 1009 DB Amsterdam, The Netherlands*
[i] *University of California Institute for Research at Particle Accelerators, Stanford, CA 94305, USA*
[j] *University of California, Riverside, CA 92521, USA*
[k] *Ames Laboratory, Iowa State University, Ames, IA 50011, USA*
[l] *University of California, Davis, CA 95616, USA*
[m] *University of Massachusetts, Amherst, MA 01003, USA*
[n] *New York University, NY 10003, USA*

Received 14 November 1986

We compare the p_T dependence of pion, kaon and proton production cross sections in the central rapidity region in e^+e^- annihilation events and in proton–proton collisions at ISR energies. We find similarities both in the p_T dependence of cross sections and in the particle composition as a function of p_T, in agreement with the hypothesis of a universal mechanism of particle production.

Both soft hadron–hadron collisions and reactions involving large momentum transfers such as e^+e^- annihilations exhibit a jet structure of the final-state hadrons as one of their most characteristic features. However, despite their similar appearance, the connection – if any – between the quark jets in e^+e^- annihilation or in lepton–nucleon reactions and the beam (or target) jets in soft hadron–hadron reactions is not all obvious. Properties of the jets in e^+e^- annihilation and of the beam jets in hadron–hadron collisions have been compared extensively [1,2]. At a given center-of-mass energy, the two types of jets exhibit similar dependencies of inclusive cross sections on the transverse momentum (p_T) of particles with respect to the jet axis, but different mean multiplicities, shapes of the multiplicity distribution and inclusive spectra. To a certain extent, differences are expected since particle production at large x will always be governed by leading particles, reminiscent of the quantum numbers of the beam particles (in hadronic collisions) or of the primary parton (in quark jets). Some of the differences can indeed be reconciled by assuming that in hadron–hadron reactions leading particles carry a sizable fraction of the availabe energy [2]. This observation suggests that in order to compare the basic mechanisms for particle production in e^+e^- annihilation and in soft hadronic collisions, one may want to concentrate on the central rapidity region, away from the fragmentation regions containing process-specific leading particles. In this paper, we present a first measurement of p_T distributions, $(1/\sigma)(d\sigma/dy dp_T^2)$, for different particle species in the central rapidity (y) region of e^+e^- annihilation events and compare it with published data for pp reactions.

The data were recorded with the TPC facility [3] at the PEP electron positron storage ring operating at 29 GeV CMS energy. The time projection chamber (TPC) was used for tracking and identification of charged particles over 87% of 4π. Data were taken with two different detector configurations: a first sample of 77 pb^{-1} with the TPC operating in a 4 kG magnetic field generated by a normal solenoid, and a more recent sample of about 70 pb^{-1} with a 13.25 kG superconducting coil. The higher field and the addition of a gating system [4] to reduce drift distortions due to space charges result in a considerable improvement in momentum resolution for the second sample, $(dp/p)^2 = (1.5\%)^2 + (0.65\%\ p)^2$ [p in GeV], as compared to $(dp/p)^2 = (6\%)^2 + (3.5\%\ p)^2$ for the first data set. Other changes in the detector hardware include installation of a new thin field cage in order to reduce the amount of material between the beam line and the TPC, and improved calibration and monitoring systems. Because of different detector acceptances and systematics, the two data sets are treated independently.

The criteria for selection of annihilation events have been described earlier [3]. Basically, an event is required to contain at least five charged-hadron tracks extrapolating to the event vertex. The sum of the energies of charged particles, ΣE, has to exceed half the beam energy, and the sum of their momentum components along the beam direction, $|\Sigma p_z|$, must not exceed 40% of ΣE. The last cut biases against hadronic events with high-energy radiative photons. Additional cuts reject τ pairs and QED events with electrons showering in the beam pipe, resulting in a sample purity of over 98%. For this analysis, only those events with an angle between beam line and sphericity axis of at least 45° are used in order to optimize the acceptance.

The cuts result in 21 434 and 20 270 multihadron events for the first and second sample, respectively. For hadrons in those events, transverse momentum p_T and rapidity y are calculated with respect to the sphericity axis. Studies with Monte Carlo two-jet $q-\bar{q}$ events (where the "real" event axis, i.e. the $q-\bar{q}$ direction, is known) show that for tracks at $y \simeq 0$ the sphericity axis gives an unbiased estimate of y and p_T.

Particles are identified by simultaneous measurement of ionization energy loss (dE/dx) and momentum. The ionization loss of each track is sampled up to 183 times, and the information is summarized by forming the mean of the 65% lowest pulse heights, resulting in a typical dE/dx resolution of 3.7% [3]. Fig. 1 shows the distribution of mean dE/dx versus momentum for tracks in multihadron events from the more recent (13.25 kG) data sample. Tracks entering this plot are required to have at least 80 measured dE/dx samples. Using its momentum and ionization energy loss measured in the TPC, and taking into account the errors on these quantities, each

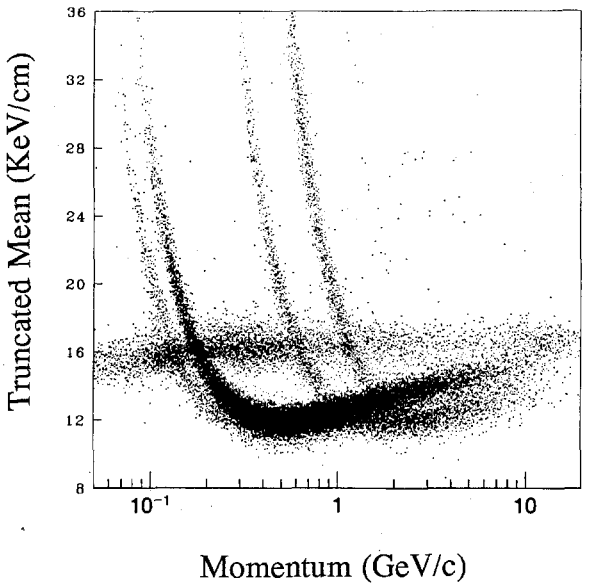

Fig. 1. Measured average ionization energy loss (65% truncated mean) versus track momentum for tracks with at least 80 measured dE/dx samples.

particle is assigned a set of χ^2's corresponding to the e, μ, π, K and p hypotheses. Based on a parameterization of particle fractions as a function of momentum and the χ^2's, probabilities for the various hypotheses are derived. A particle is considered identifiable, if it has a well-measured momentum, at least 40 dE/dx samples, and if one of the probabilities exceeds 70%. Depending on their momentum, 80% to >95% of all particles are correctly identified using these criteria. An unfolding technique is then used to correct for mislabeled particles. To derive e.g. the K cross section, we count the number M_i of particles identified as "i" in a given p_T and y bin (where y is calculated assuming K masses). Here i stands for $e^\pm$, $\mu^\pm$, $\pi^\pm$, $K^\pm$ or p, $\bar{p}$. Let R_i be the real number of identifiable particles of type i. Then $M_i = \sum C_{ij} R_j$, where C_{ij} is the probability to identify a particle of type j as a particle of type i. The C_{ij} are evaluated using a Monte Carlo simulation of the detector. Their values are determined mainly by the dE/dx resolution and by the separation of the mean dE/dx of two species at a given momentum; the Monte Carlo simulation is used only to average the C_{ij} over the momentum spectra for a given y, p_T bin.

For any given bin, the numbers R_j are now calculated by inverting the matrix equation, $R = C^{-1}M$. Since over most of the phase space π and μ cannot be separated, π's and μ's are lumped together at this stage; in the following, so-called π cross sections actually refer to the sum of π and μ. However, the μ contribution to the cross section is typically small compared to the errors assigned to the cross section. Appropriate statistical and systematic errors are assigned to the matrix elements and are propagated through the matrix inversion. A Monte Carlo derived acceptance finally relates the number of identifiable particles of a given species to the number of particles produced at the vertex. Corrections for the bias introduced by the event selection criteria and for the effects of initial state radiation are included in this factor. In order not to be limited by sizable uncertainties in the p cross section due to secondary protons created in interactions of primary hadrons in the beam pipe, we actually use only negative-particle cross sections and assume charge symmetry. The low-field and high-field data sets prove to be consistent after (separate) acceptance corrections and combine the results.

Fig. 2 shows the inclusive $\pi^\pm$ (a), $K^\pm$ (b) and p, $\bar{p}$ (c) cross sections, $(1/\sigma)(d\sigma/d|y|dp_T^2)$, at $y \simeq 0$ as a function of p_T, for e^+e^- annihilation events at $\sqrt{s} = 29$ GeV and for proton–proton interactions. We use ISR data at $\sqrt{s} = 53$ GeV [5] – the highest energy where detailed pp data are available – for our comparison, since pp collisions at 53 GeV and e^+e^{-1} events at 29 GeV result in similar effective energies of the hadronic system, once leading hadrons are removed. For e^+e^- events p_T and y are defined with respect to the sphericity axis. In the pp reaction, y and p_T refer to the proton–proton collision axis. The cross section displayed in fig. 2 represents the number of particles per hadronic event, that is, the inclusive cross section normalized to the total cross section. Whereas the normalization factor $(1/\sigma)$ is well-defined in the e^+e^- case, it is not so clear which cross section should be used in pp reactions. We used the non-diffractive cross section[‡1], since diffractive events will typically contribute few particles at $y = 0$.

The ISR data refer to a narrow y window close to $y = 0$, whereas the e^+e^- data are averaged over the

[‡1] The non-diffractive cross section is estimated using a compilation from ref. [6].

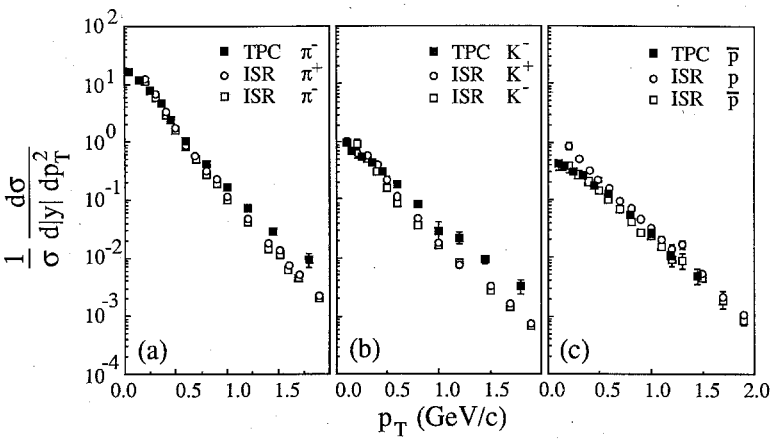

Fig. 2. (a) Full squares: cross section $(1/\sigma)(d\sigma/d|y|dp_T^2)$ for π^- production in e^+e^- annihilation at $\sqrt{s}=29$ GeV, as a function of p_T, for $|y|<1$. Error bars include systematic errors. Open circles and open squares: π^+ and π^- production cross sections, respectively, in pp collisions at $\sqrt{s}=53$ GeV, for $y\simeq 0$, from ref. [5]. See text for discussion of systematic errors on pp data. (b) Full squares: K^- cross section in e^+e^- annihilation; open circles and open squares: K^+ and K^- cross section in pp reactions [5]. (c) Full squares: $\bar{p}$ cross section in e^+e^- annihilation; open circles and open squares: p and $\bar{p}$ cross section in pp reactions [5].

interval $0<|y|<1$, a region in which cross sections are nearly independent of rapidity. According to the Lund fragmentation model for e^+e^- annihilation [7], at low p_T less than 10% of the particles of each species in that y region are leading ("rank-one") particles in the sense that they contain the primary quark or antiquark, or are decay products of a rank-one hadron. Measurements [8] of the ratio of flavor-singlet to non-singlet fragmentation functions support this prediction. At higher p_T, above 1 GeV, contributions of charm and bottom decays to the π and K rates are non-negligible and account for 25–40% of the cross section. For proton–proton collisions, the contributions of proton valence quarks to particle production in the central region can be estimated from the charge asymmetry between positive and negative hadrons. For pions (fig. 2a) and kaons (fig. 2b), positive and negative rates agree within 20%, indicating that mesons at $y\simeq 0$ have little memory of the positive charges of the incident protons. Proton and antiproton cross sections, however, differ significantly (fig. 2c). This is an indication that, due to the low number of additional baryon–antibaryon pairs produced in typical interactions, the contribution of p's spilling from the forward and backward fragmentation regions into the central region is not negligible, and that the $\bar{p}$ cross sections should be used for the comparison.

We note that whereas errors given for the TPC data include systematic uncertainties, the ISR data show only statistical errors and uncertainties in the luminosity measurement. Additional systematic errors e.g. due to uncertainties in the absorption corrections are particularly large for $\bar{p}$ cross sections above 1 GeV/c, where a high-pressure Čerenkov counter was used to identify particles. Comparison of ISR data at $\sqrt{s}=23$ GeV [5] with high-precision FNAL data [9] indicate that in this regions the errors may even exceed the quoted 30% additional uncertainty. Finally, one should note that even at $y\simeq 0$ about 10% of the production cross section may be due to diffractive processes.

We see from fig. 2 that at low p_T, where non-perturbative processes are expected to dominate particle production, $\pi^\pm$, $K^\pm$ and $\bar{p}$ cross sections from e^+e^- annihilation and from inelastic pp reactions are quite similar both in shape and in magnitude. At p_T values large compared to the average p_T of about 0.4 GeV/c, pp data fall below the e^+e^- cross sections. At those p_T, particle production is governed by hard processes such as gluon–gluon and quark–gluon scattering (with an intrinsic p_T^{-4} dependence) in hadronic reactions, and by hard-gluon emission (with an intrinsic p_T^{-2} dependence) as well as by heavy-quark decays in e^+e^- reactions; hence we expect to see differences increasing with p_T. The similarities at low

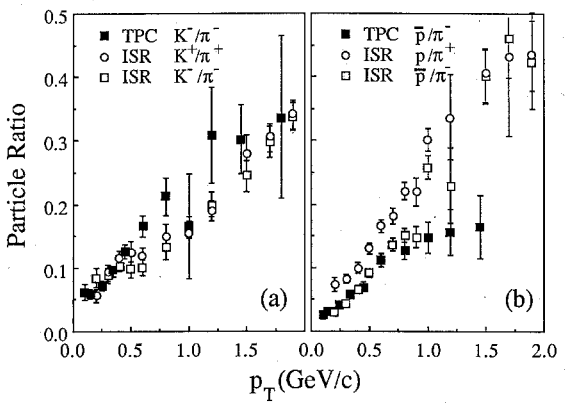

Fig. 3. (a) Ratio of production cross sections at $y \simeq 0$, as a function of p_T. Full squares: e^+e^- data on K^-/π^- at $\sqrt{s}=29$ GeV; open circles and open squares: pp data on K^+/π^+ and K^-/π^-, respectively, at $\sqrt{s}=53$ GeV [5]. (b) Full squares: e^+e^- data on $\bar{p}/\pi^-$; open circles and open squares: pp data on p/π^+ and $\bar{p}/\pi^-$, respectively [5].

p_T between the two types of reactions are emphasized in fig. 3, where the K/π (fig. 3a) and p, $\bar{p}/\pi$ (fig. 3b) ratios are compared. In both reactions, the fraction of heavy particles rises significantly with increasing p_T.

The similarity in the p_T dependence of cross sections and particle ratios is predicted by a number of hadronization models, most notably the Lund model [10] and dual or multiple chain models [11][‡2]. In these models, the primary proton–proton interaction is assumed to liberate color-triplet sources (quarks) or color-antitriplet sources (diquark systems). Fluxtubes ("strings" or "chains") are spanned between triplets in one proton and antitriplets in the other. These fluxtubes have little transverse momentum and hadronize just like the color triplet–antitriplet system created e^+e^- annihilation into quarks. They exhibit therefore identical particle composition and p_T spectra, provided that one looks at the central region, away from the forward regions containing diquark remnants in pp collisions, or possibly heavy quark decays in e^+e^- reactions. Since the energies of the initial protons are shared by two or more such strings, as compared to a single one in e^+e^- annihilation, inclusive spectra, mean multiplicities and multiplicity distributions are indeed expected to differ [11,12]. The agreement of e^+e^- and pp cross sections $(1/\sigma)(d\sigma/d|y|d\,p_T^2)$ at $y \simeq 0$ not only in shape, but also in normalization, is explained as due to the incomplete overlap of the multiple chains in hadronic reactions [11,12].

[‡2] For a recent summary and references see ref. [12].

We acknowledge the efforts of the PEP staff, and the engineers, programmers and technicians who made this work possible. This work was supported by the US Department of Energy, by the National Science Foundation and by the Joint Japan–US Collaboration in High Energy Physics.

References

[1] A. Breakstone et al., Z. Phys. C 11 (1981) 203;
HRS Collab., D. Bender et al., Phys. Rev. D 31 (1985) 1;
TASSO Collab., M. Althoff et al., Z. Phys. C 22 (1984) 307.
[2] M. Basile et al., Nuovo Cimento A 79 (1984) 1; Nuovo Cimento Lett. 41 (1984) 293.
[3] TPC Collab., A. Aihara et al., Phys. Rev. Lett. 52 (1984) 577.
[4] P. Nemethy et al., Nucl. Instrum. Methods 212 (1983) 273.
[5] British–Scandinavian Collab., B. Alper et al., Nucl. Phys. B 100 (1975) 237.
[6] K. Fialkowski and H.I. Miettinen, Nucl. Phys. B 103 (1976) 247.
[7] B. Andersson et al., Phys. Rep. 97 (1983) 31;
T. Sjöstrand, Comput. Phys. Commun. 27 (1982) 243; 28 (1983) 229.
[8] TPC Collab., A. Aihara et al., Z. Phys. C 27 (1985) 495.
[9] D. Antreasyan et al., Phys. Rev. D 19 (1979) 764.
[10] B. Andersson, G. Gustafson and C. Peterson, Phys. Lett. B 69 (1977) 221; B 71 (1977) 337;
H.U. Bengtsson and G. Ingelman, Comput. Phys. Commun. 34 (1985) 251.
[11] A. Capella, U. Sukhatme and J. Tran Thanh Van, Z. Phys. C 3 (1980) 329.
[12] E.g. P. Aurenche, F.W. Bopp and J. Ranft, Z. Phys. C 23 (1984) 67;
J. Ranft and S. Ritter, Z. Phys. C 27 (1985) 413.